P8A.8 DROP SHAPE AND ORIENTATION ANGLE DISTRIBUTIONS IN RAIN FROM 2-D VIDEO DISDROMETER

G.J. Huang[1], V. N. Bringi[1*], M. Schönhuber[2], M. Thurai[1], T. Shimomai[3], T. Kozu[3], Marzuki[4] and W. Harjupa[5]

[1]Colorado State University, Fort Collins, Colorado, USA
[2]Joanneum Research, Graz, Austria
[3]Shimane University, Matsue, Japan
[4]Andalas University, Padang, Indonesia
[5]LAPAN, Bukittingi, Indonesia

1. INTRODUCTION

Drop shapes and orientation angles are two factors which govern the relationships between various parameters involved in the rainfall estimation from polarimetric radar data. They also govern the relationships required for attenuation correction schemes which may need to be applied, particularly for C-band and higher frequencies (Bringi and Chandrasekar 2001).

In an earlier study, the drop shapes were investigated using the 2-D video disdrometer (2DVD; Randeu et al 2002, Kruger and Krajewski, 2002) in artificial rain (Thurai and Bringi, 2005). Contoured shapes (which filters the quantization noise of the instrument) were derived for over 115,000 drops (Thurai et al, 2007) and were shown to be consistent with the Beard-Chuang (non-oblate) shape model (1987). Drops with equivalent diameter (D_{eq}) greater than 4 mm were shown to deviate more and more from oblate shapes. A fitted equation for the mean shapes was derived based only on D_{eq}.

In this study, we compare the fitted equation with the contoured shapes in natural rain, derived once again from 2DVD. Data from two different sites are used in the comparisons, one from a sub-tropical oceanic site (Okinawa, Japan) and the other from an equatorial region in Indonesia (Koto Tabang). We also report on the preliminary results of orientation angles derived from the two sites as well as the artificial rain experiment conducted earlier.

We also report on the preliminary results of orientation angles (θ, Φ: zenith and azimuth angles, respectively) derived from the canting angles obtained from the two camera images. The data set is from the 80 m fall bridge experiment referred to earlier. Since these data were obtained under calm wind conditions, the orientation angle distributions form a 'baseline' which may be compared with natural rain.

*Corresponding author address: V. N. Bringi, Dept. of Electrical Engineering, Colorado State University, Fort Collins, CO 80523-1373, USA.
Email: bringi@engr.colostate.edu

Previously the algorithm for deriving (θ, Φ) has been described in (Schoenhuber et al 2000; Schauer 1998) and applied to drops > 3.5 mm under (a) artificial rain conditions (35 m fall) and (b) for a (low wind) natural rain event from Papua-new Guinea. They found that the mean zenith angle under calm conditions was close to 5^o. Later, the algorithm was further developed by Joanneum Research to allow orientation angles to be derived for drops > 2 mm (later 2DVD units were equipped with higher speed cameras which reduced the quantization noise).

2. CONTOURED SHAPES AND EQUATIONS

The earlier study (Thurai et al 2007) on drop shapes in artificial rain experiment derived the so-called 'probability contours' for various values of D_{eq}. The 'mean' contours were then fitted to a D_{eq} dependent equation, given by a smoothed conical function, as follows:

$$x = c_1\sqrt{1-\left(\frac{y}{c_2}\right)^2}\left[\cos^{-1}\left(\frac{y}{c_3 c_2}\right)\right]\left[c_4\left(\frac{y}{c_2}\right)^2+1\right] \quad (1)$$

where x and y are the Cartesian coordinates and the parameters c_1, c_2, c_3 and c_4 were fitted to obtain the mean dependence on the D_{eq} (in mm), given by:

$$c_1 = \frac{1}{\pi}\left(0.02914 D_{eq}^2 + 0.9263 D_{eq} + 0.07791\right)$$

$$c_2 = -0.01938 D_{eq}^2 + 0.4698 D_{eq} + 0.09538$$

$$c_3 = -0.06123 D_{eq}^3 + 1.3880 D_{eq}^2 - 10.41 D_{eq} + 28.34$$

$$c_4 = -0.01352 D_{eq}^3 + 0.2014 D_{eq}^2 - 0.8964 D_{eq} + 1.226 \quad \text{for } D_{eq} > 4\,mm$$

$$c_4 = 0 \quad \text{for } 1.5 \le D_{eq} \le 4\,mm$$

Eq. (1) is modified/enhanced version of the equation given in Wang (1982). The parameters c_1, c_2 and c_3 are the same as *a*, *c* and λ respectively in Wang (1982). The term containing c_4 is an additional term required to represent the mean shapes for drops

larger than 4 mm whose base becomes increasingly flatter with larger size. Fig. 1 shows the mean contours derived from eq. (1) for D_{eq} up to 6 mm.

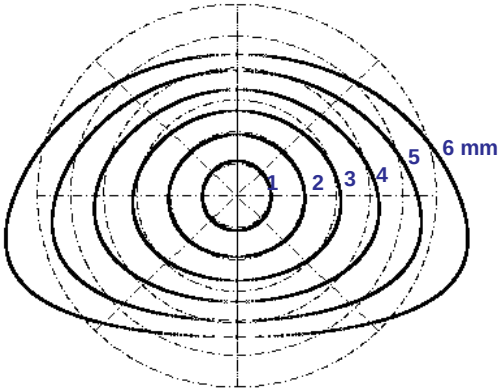

Fig. 1: 2DVD (processed) image - based mean shapes for D_{eq} up to 6 mm, given by eq. (1)

3. NATURAL RAIN DATA

3.1 Probability contours and dimensions

Fig. 2(a) and 2(b) show the curves from eq. (1) for 3 and 4 mm drops, superimposed on the probability contours derived from the 2DVD data taken in Okinawa, a sub-tropical oceanic site. The data were taken during a long duration 'Baiu' event.

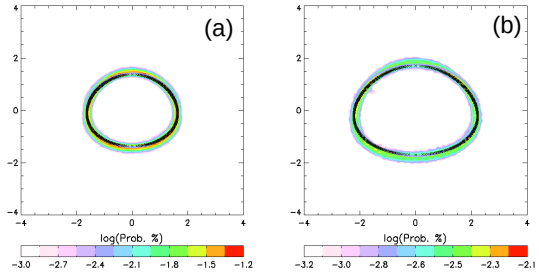

Fig. 2: Drop shape probability contours (color intensity) and fitted equations to the mean shapes (black line) given for D_{eq} in the range 3-3.25 mm (left) and 4-4.25 mm (right) from the 2DVD data in Okinawa (Bringi et al 2006).

The color intensity represents the variation in drop shapes due to drop oscillations. Fig. 3 shows the extent of these oscillations derived from the 2DVD data at the '95% probable' limits for the 4 mm drop. The vertical limit ranges from 2.6 to 4.1 mm whilst the horizontal limit ranges from 3.8 to 4.9 mm. Compared with the mean dimensions of 3.35 mm vertical and 4.4 mm horizontal, the limits suggest that shape variation occurs more in the vertical (particularly at the top) than horizontal and hence a more reasonable term to describe the oscillation mode would be 'oblate-conical' rather than 'oblate-prolate'.

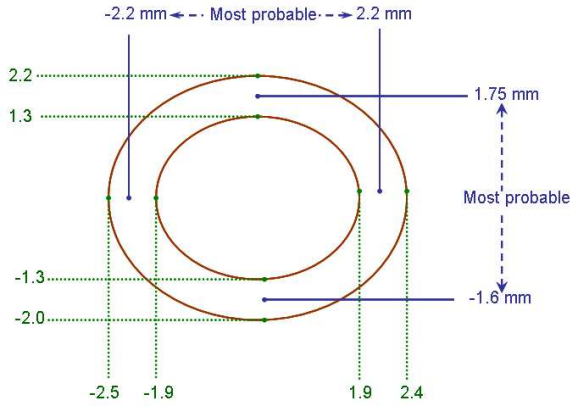

Fig. 3: Contour limits for the 4 mm drop given in terms of the 95% probability level (inner and outer curves). The variation is seen to occur more in the vertical than in the horozintal. Moreover, the vertical variation is somewhat higher at the top, thus indicating that the oscillation mode should be more appropraitely termed oblate-conical rather than oblate-prolate.

3.2 Oblate approximation

For drops smaller than 4 mm, eq. (1) contains only three D_{eq} dependent terms, i.e. c_1, c_2 and c_3 and their shapes, to a large extent, could be approximated to oblate spheroids, with axis ratios given by Thurai et al (2007):

$$\frac{b}{a} = 1.065 - 6.25\times10^{-2}\left(D_{eq}\right) - 3.99\times10^{-3}\left(D_{eq}^2\right) + 7.66\times10^{-4}\left(D_{eq}^3\right) - 4.095\times10^{-5}\left(D_{eq}^4\right) \quad for\ D_{eq} > 1.5\,mm \qquad (2a)$$

Note, eq. (2a) is a re-fitted equation to the results obtained by Thurai and Bringi, 2005. For drops smaller than 1.5 mm, the finite resolution of the 2DVD does not allow their axis ratios to be accurately derived; hence for calculation purposes, the laboratory data by Beard and Kubesh (1991) are used for 0.7 ≤ D_{eq} ≤ 1.5 mm. Below 0.7 mm, drops are assumed spherial. For completion, the axis ratio equations for small drops are given below:

$$\frac{b}{a} = 1.17 - 0.516\left(D_{eq}\right) + 0.47\left(D_{eq}^2\right) - 0.132\left(D_{eq}^3\right) - 8.5\times10^{-3}\left(D_{eq}^4\right) \quad for\ 0.7 \le D_{eq} \le 1.5\,mm \qquad (2b)$$

$$\frac{b}{a} = 1 \quad for\ \ D_{eq} < 0.7\,mm \qquad (2c)$$

3.3 2DVD data from Western Sumatra

In the recent months, it became possible to accurately calibrate a (high-profile) 2DVD located in Koto Tabang in Sumatra in Indonesia (Kozu et al. 2005). The site has several atmospheric remote sensing instruments and has been included in a comparative study on rain drop size distributions in various tropical climates and their seasonal and diurnal variations (Kozu et al, 2006). Since then, the 2DVD underwent extensive calibrations in order to derive accurate drop shape information. Soon after these calibrations (in March 2007), there were several days with high intensity rainfall as part of the pre-SW monsoon season. Fortunately, the rainfall events were not affected by high wind effects and hence any consequent distortions were minimal. Fig. 4 shows the axis ratio variations for various diameter intervals, taken during three events in this season. Superimposed on the color intensity plot is the axis ratio variation given by the oblate approximate versions given in eq. (2a) above for $D_{eq} \geq 1.5$ mm and eq. (2b) for $1 < D_{eq} < 1.5$ mm. The agreement is good, since the fitted equations 'run' through the mode of the measured axis ratio distributions, at least for D_{eq} up to 3 mm, beyond which there were insufficient number of drops.

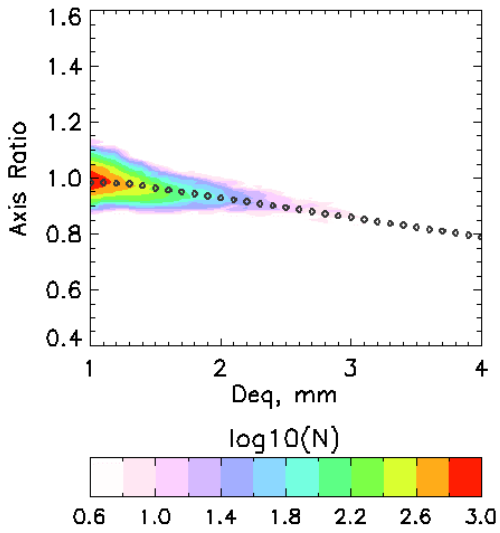

Fig. 4: Intensity plots of axis ratio distributions as a function of drop diameter from the (well-calibrated) 2DVD data taken over three events during the 2007 pre-SW monsoon period in Koto Tabang, western Sumatra, Indonesia. The color indicates $\log_{10}$ of the number of drops.

Fig. 5 compares the axis ratio distributions for the drop equivalent diameters ranging in the 2-2.5 mm interval from the Sumatra data with those from the artifical rain experiment (Thurai and Bringi, 2005). The two curves lie close to each other and are similar in terms of their distributions.

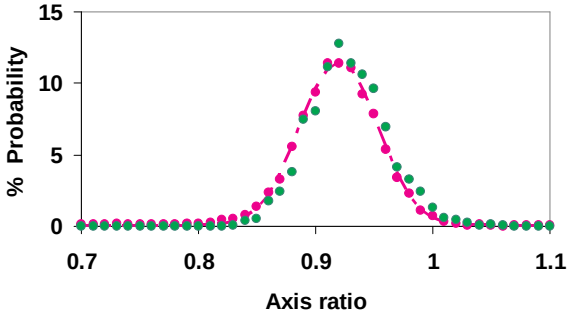

Fig. 5: Axis ratio distribution shown in green for 2-2.5 mm diameter interval for the Sumatra data from Fig. 4. The majenta points are the refernce data from the artificial rain experiment (Thurai and Bringi, 2005).

From the three events used in this study so far, there were sufficient number of drops (just over 200) in the 3-3.5 mm drop diameter interval to derive the shape probability contour using both camera views. This is shown in fig. 6. The black curve, once again representing eq. (1) above, fits well with the maximum probability values within the color intensity plot. It seems that the equilibrium shape given in eq. (1) is a good representation of the 3 mm drops falling under relatively calm condictions, even in an equatorial region such as Koto Tabang.

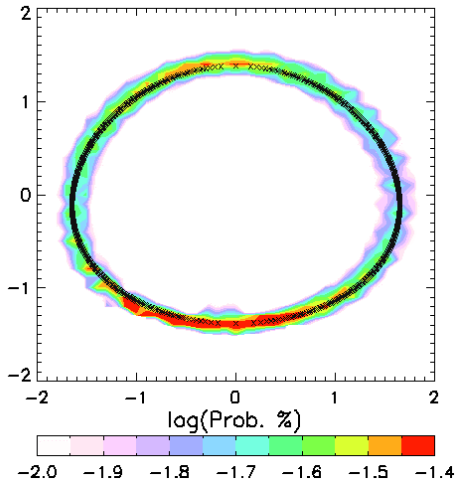

Fig. 6: Shape probability contour for the drops in the 3-3.25 mm range from the 2DVD data taken in Sumatra. Superimposed in black is the contour using eq. (1), representing the mean shape derived from the artificial rain experiment (Thurai et al 2007).

There are several other events in April 2007 which were recorded under relatively low wind conditions. It is the intention of the authors to extend the analysis to include these additional events, some of which have produced drops larger than 4 mm.

4. ORIENTATION ANGLE DISTRIBUTIONS

When developing dual-polarized radar alogrithms for rain rate or DSD parameter retrievals using Z_{dr} and/or K_{dp}, the assumption is often made that the canting angle (β) distribution in the plane of polarization is Gaussian with zero mean and standard deviation (σ_β) of 5-10^o (Beard and Jameson 1984 argue that σ_β should be < 5^o due to turbulence effects). The canting angle is the angle between the projection of the drop's symmetry axis on the polarization plane and the projection of the local vertical direction on this same plane (e.g., Holt 1984).

The orientation of the symmetry axis of a spheroid in 3D is defined by its zenith or polar angle (θ) and its azimuth angle (Φ). As such the orientation distribution of the symmetry axis is described on a spherical surface, i.e., p(Ω) dΩ gives the probability that the symmetry axis lies within the solid angle interval (Ω, Ω+ dΩ) and the Fisher distributions (Mardia 1972) are appropriate on a spherical surface as opposed to assuming apriori the Gaussian shape (see Section 2.3.6 of Bringi and Chandrasekar 2001). The previously defined canting angle (β) can be derived from (θ, Φ) and the radar elevation angle (usually assumed to be 0). It Is also common to assume that the pdf of Φ is uniform in the interval (0,2π). In which case the marginal pdf of θ, or $p_\Omega(\theta) = p(\theta)\,\mathrm{Sin}\,\theta$ is not Gaussian (see Fig. 2.9a of Bringi and Chandrasekar 2001). However, p(θ) may be assumed to be Gaussian (mean θ = 0; σ_θ) in which case p(β) will also be Gaussian with mean=0 and $\sigma_\beta \approx \sigma_\theta$. Simulations have shown this to be valid for σ_θ at least up to 25^o (Huang 2003).

The 2D video disdrometer has two, orthogonally placed line scan cameras which give two 'views' of the raindrop as it passes through the sensor area. If the drops fall vertically through the 2 light planes (typical plane separation is around 6 mm), the canting angle is 0. This is true even if the drop has a horizontal velocity component. However, if the drop is canted as it enters the sensor area then the 'distorted' image is more difficult to 'correct' for which is a precursor step to determining the 'true' canting angle (the details are given in Schoenhuber et al 2000; Schauer 1998). Here, the term canting angle is used (even though it is defined for radar applications) since each camera image can be thought of as being in the 'polarization' plane of a radar beam at zero elevation angle. As such, two canting angles are derived for each drop (the angle being defined from the vertical line which is perpendicular to the light planes).

For all drops with $D_{eq} \geq 2$ mm from the 80 m fall bridge experiment (Thurai and Bringi, 2005, Thurai et al, 2007), the histograms of canting angles derived from Camera A and Camera B are shown in Figs. 7a,b. Note that the shape of the canting angle histograms are approximately Gaussian with mean $\beta \approx 0$ and σ_β of around 7^o. The marginal pdf $p_\Omega(\theta)$ derived from the two canting angles is shown as a histogram in Fig. 8. Note that shape is not Gaussian, rather it is skewed with mode of $\theta \approx 3^o$. The corresponding marginal pdf p(Φ) is shown as a histogram in Fig. 9. Ignoring the 'multi-modes' which occur at regular intervals of 45^o (most likely due to the algorithm), the shape of the histogram suggests a uniform pdf in the range 0-2π.

Further, for each drop class diameter interval from 2-7 mm (with bin width of 0.5 mm), the σ_θ was calculated as a function of the mid-point of the diameter class and is shown in Fig. 10. Note how the σ_θ falls with increase in D_{eq}, the inference being that the larger drops are more stably oriented than the small ones. From these data σ_θ reduces from 6.8^o at 2 mm to 4.8^o at 7 mm. These results support the dual-polarized radar observations made by Huang et al (2003) who derived the mean variation of σ_β as a function of Z_{dr} in a summer-time convective rain storm in Colorado using the CSU-CHILL radar. Their Fig. 2 from that conference paper is reproduced in Fig. 11 (for details of the methodology please refer to Huang et al 2003). They comment " …that σ_β decreases with Z_{dr} and reflects the fact that larger drops are more stably oriented as compared to small-sized drops". The 2D video estimation of orientation angle distributions from the 80 m fall bridge experiments under calm conditions is consistent with the radar-based results of Huang et al (2003).

5. SUMMARY

We have examined drop shapes in natural rain from two different climate regimes. The first one is a subtropical oceanic site and the data examined were taken during a long duration 'Baiu' event with somewhat high winds. The probability contour plots derived from these dataset show small amount of deviation from our equilibrium drop shapes obtained from the artificial rain experiment, at least for the 4 mm drops. Dimensions of the limits of the contours (inner and outer) show that the shape variation occurs more in the vertical than in the horozintal. Moreover, the vertical variation is somewhat higher at the top, thus indicating that the oscillation mode should be more appropriately termed oblate-conical rather than oblate-prolate.

The second site is located in an equatorial region and a limited amount of dataset became available (at the time of writing this article), after meticulous calibratation procedures, during the pre-SW monsoon period, with very little wind speeds. Axis ratios show very similar distributions to the artificial rain results. Moreover, the shape probability contour for the 3 mm drops matches the mean artificial rain contour very well, thus implying that the latter can represent the equilibrium drop shapes prevalent in natural rain.

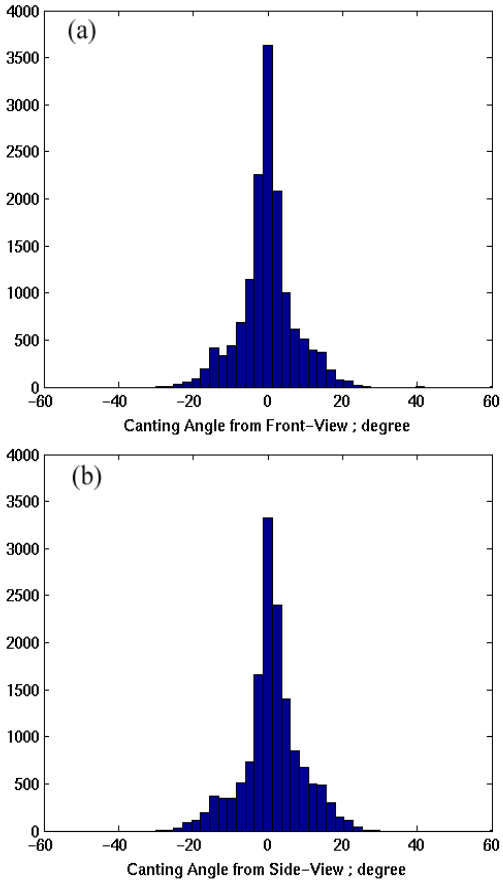

Fig. 7a,b: Histograms of canting angles from front (camera A) and side (camera B) views. Note that they were almost symmetric with mean of 0^o with standard deviation 7.2^o and 7.8^o, respectively.

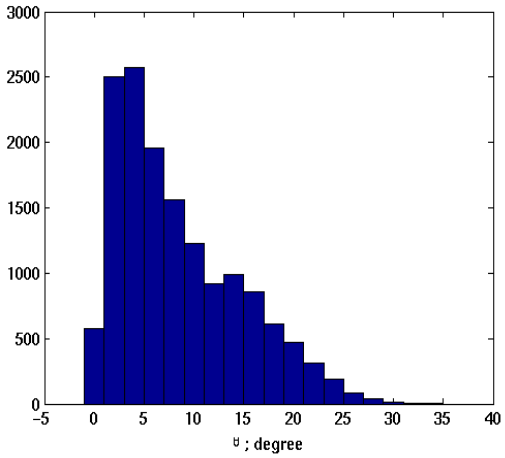

Fig. 8: Histogram of zenith angle (θ) derived from the two canting angle distributions in Fig. 7. It represents the marginal pdf $p_\Omega(\theta)$.

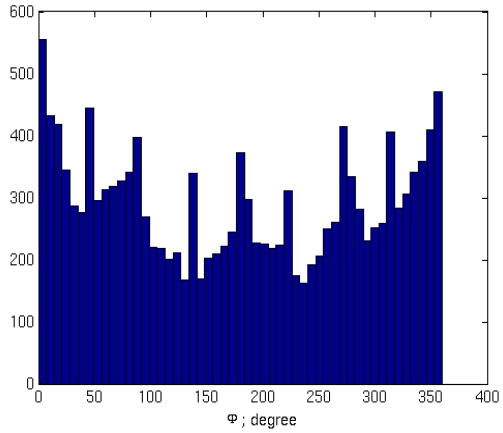

Fig. 9: Histogram of azimuth angles (Φ). It is close to being uniformly distributed between (0, 2π). The 'multi-modes' at approximately 45^o spacing may be due to the algorithm.

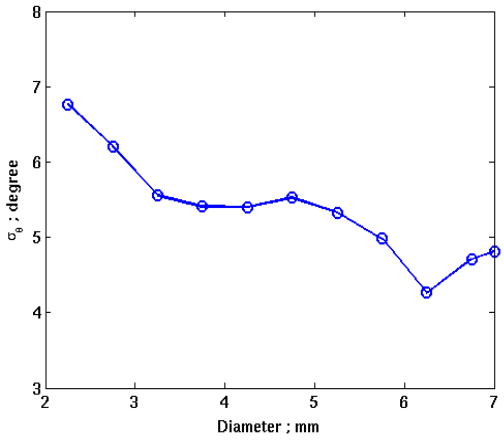

Fig. 10: Standard deviation of θ vs. drop size (D_{eq}) from the 80 m fall bridge experiment. The size intervals are from 2 to 7mm with 0.5 mm step. The last data point represents those drops greater than 7 mm. Note that in calm conditions prevalent during the experiment, the large drops are more stably oriented (smaller σ_θ) than small drops (larger σ_θ).

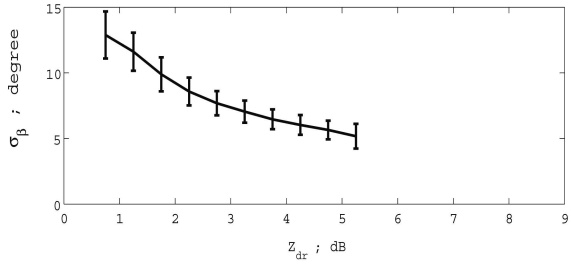

Fig. 11: The mean σ_β vs. Z_{dr} from 11 June, 2000 convective rain event from STEPS. The data are from a number of PPI sweeps using the CSU-CHILL radar. The vertical bars are mean ± σ.

From the distributions of the canting angles derived from the orthogonal views of drops > 2 mm from the 80 m fall artificial rain experiment under calm conditions, we were able to deduce the distributions of the zenith and azimuth angles. The azimuthal angle distribution was more or less uniform in the range (0,2π) while the distribution of p_Ω (θ)= p(θ) Sin θ was as expected similar to the Fisher distribution. The mean of the standard deviation of the histogram representing p_Ω (θ) was shown to decrease with D_{eq} implying that larger drops are more stably oriented than the smaller ones. This is in agreement with previous radar-based results of standard deviation of the canting angle decreasing with increasing Z_{dr}. We will analyze the orientation distributions in natural rain under light wind conditions in the near future.

ACKNOWLEDGEMENTS

This work was supported by the US National Science Foundation via grant ATM-0603720. The Okinawa data were kindly supplied by Dr. K. Nakagawa at NICT of Japan.

REFERENCES

Beard, K.V. and A.R. Jameson, 1984: Raindrop canting, J. Atmos. Sci., vol. 40, 448-454.

Bringi, V.N. and V. Chandrasekar, 2001: Polarization Doppler weather radar, Cambridge University Press, pp 636.

Bringi, V.N., M. Thurai, K. Nakagawa, G. J. Huang, T. Kobayashi, A. Adachi, H. Hanado, and S. Sekizawa, 2006: Rainfall estimation from C-band polarimetric radar in Okinawa, Japan: Comparisons with 2D-video disdrometer and 400 MHz wind profiler, J. Meteor. Soc. Japan, vol. **84**, 705–724.

Holt, A.R., 1984: Some factors affecting the remote sensing of rain by polarization diversity radar in the 3- to-35 GHz range, Radio Sci., vol. 19, 1399-1412.

Huang, G.J., 2003: Evaluation and application of polarimetric radar data for the measurement of rainfall. PhD dissertation, Colorado State University.

Huang, G.J., V.N. Bringi and J. Hubbert, 2003: An algorithm for estimating the variance of the canting angle distribution using polarimetric covariance matrix data, 31st Conf. on Radar Meteor., 6-12 August, Seattle, WA.

Kozu, T., T. Shimomai, Z. Akramin, Marzuki, Y. Shibagaki and H. Hashiguchi, 2005: Intraseasonal variation of raindrop size distribution at Koto Tabang, West Sumatra, Indonesia, Geophys. Res. Lett., **32**, L07803, doi:10.1029/2004GL022340.

Kozu, T., K.K. Reddy, S. Mori, M. Thurai, J.T. Ong, D.N. Rao and T. Shimomai, 2006: Seasonal and Diurnal Variations of Raindrop Size Distribution in Asian Monsoon Region, J. Meteorol. Soc. Japan, **84A**, 195-209

Kruger, A., and W. F. Krajewski, 2002: Two-dimensional video disdrometer: A description. J. Atmos. Oceanic Technol., vol. **19**, 602–617.

Mardia, K.V., 1972: Statistics of Directional Data, Academic press, N.Y.

Randeu, W. L., M. Schönhuber, and G. Lammer, 2002: Real-time measurements and analyses of precipitation micro-structure and dynamics, Proc. 2nd European Conf. Radar Meteor. (ERAD), Delft, Netherlands, Copernicus GmbH, European Meteor. Soc., Proc. ISBN-3-936586-04-7, 78–83.

Schauer, G, 1998: Distrometer-based determination of precipitation parameters for wave propagation research, Diploma Thesis, Technical Univ. of Graz (Supervisors: W.L. Randeu and M. Schoenhuber), pp 98.

Schoenhuber, M., W.L. Randeu, H.E. Urban and J.P.V. Poiares Baptista, 2000: Field measurements of raindrop orientation angles, AP Milleneum Conf. Ant. Prop., Davos, Switzerland, 9-16 April.

Thurai, M. and V.N. Bringi, 2005: Drop Axis Ratios from 2D Video Disdrometer, J Atmos Ocean Tech, vol. **22**, 963–975.

Thurai, M., G.J. Huang, V.N. Bringi, W. L. Randeu and M. Schönhuber, 2007: Drop Shapes, Model Comparisons, and Calculations of Polarimetric Radar Parameters in Rain, J. Atmos. Ocean. Tech., **24,** (6), 1019-1032.